Commercial HPWH with Natural Gas Backup

Joseph Rendall, Borui Cui, and Helia Zandi Oak Ridge National Laboratory

ABSTRACT

A hybrid high performance water heater (HPWH) system with natural gas water heater (NGWH) backup, to handle the centralized recirculation heat losses, was implemented in a commercial building on the Oak Ridge National Laboratory (ORNL) campus. The building the water heater served was an office space with over 500 occupants, five floors, 44 laboratory spaces, 18 conference rooms/auditoriums, and 24 restrooms. The centralized water heating system employs air-source HPWHs, which extract heat from the mechanical room space. The room houses two large boilers (2 MMBtu/hr each), and the heat lost from their shells is sufficient to meet the building's average domestic hot water needs. Thus, two air-source HPWHs with a capacity of 90 kBtu/hr pull heat from the space and were paired with two NGWHs (200 kBtu/hr) equipped with 110-gallon storage, ensuring the base load is handled by the HPWHs while enabling the NGWH to handle the recirculation heat losses and provide rapid heating during peak demands. To evaluate system performance, the setup includes five ultrasonic flow meters with temperature sensors, 16 surface-mounted thermocouples, and two energy meters for the HPWHs. Data acquisition is managed by the building energy management system, with measurements also aiding validation of ORNL's centralized water heating model. The project explores affordable and minimally invasive methods for determining accurate energy balances in commercial water heating systems. Preliminary results indicate the system's reliability and affordability, with projected savings of at least 60% in operational costs compared to HPWH systems with electric resistance backup that handles the recirculation heat losses.

Introduction

This modelling, monitoring, and validation project was conducted at Oak Ridge National Laboratory (ORNL) in Tennessee. The building receives electricity from the Tennessee Valley Authority (TVA). The study site is a five-story commercial office building with over 500 occupants and includes 44 laboratory spaces, 18 conference rooms/auditoriums, and 24 restrooms. The hybrid water-heating system and all monitoring equipment were installed in the building's boiler (mechanical) room, which also houses large natural gas boilers used for space heating.

High performance water heaters (HPWH) conversions, that use advanced vapor compressions cycles, in existing buildings are an important part of many energy saving plans for

Notice: This manuscript has been authored by UT-Battelle, LLC, under contract DE-AC05-00OR22725 with the US Department of Energy (DOE). The US government retains and the publisher, by accepting the article for publication, acknowledges that the US government retains a nonexclusive, paid-up, irrevocable, worldwide license to publish or reproduce the published form of this manuscript, or allow others to do so, for US government purposes. DOE will provide public access to these results of federally sponsored research in accordance with the DOE Public Access Plan (http://energy.gov/downloads/doe-public-access-plan).

metropolitan areas around the United States (Steven Winters Associates Inc. 2019). Buildings with centralized water heating HPWHs typically rely on a back-up water heater, sometimes called a swing tank or maintenance tank, to manage recirculation heat losses in centralized water heating plants (NEEA 2024). Recirculation losses can significantly increase energy demand, potentially doubling water heating costs while relying on low-performing electric resistance heaters. To address this, the hybrid system design integrated high-capacity NGWHs to meet recirculation demands and handle peak large-scale hot water usage.

The objective of this project was to evaluate the performance of a hybrid system configuration integrating natural gas water heaters (NGWHs) and high-performance water heaters (HPWHs) for water heating in commercial buildings. The study focuses on optimizing low-cost system operation and determining cost-effective monitoring methods for centralized water heating systems. The placement of the air-source HPWHs inside a boiler room ensured a high coefficient of performance (COP) during winter operation.

The study also examined the impact of piping configurations on HPWH performance in centralized systems. The installed HPWHs incorporated piping for both parallel and series configurations with storage tanks backed up by NGWHs. Preliminary results indicate the system configuration achieves at least a 60% cost reduction compared to conventional HPWH systems relying on electric resistance backup. Additionally, the project aimed to develop an affordable and nonintrusive method to establish accurate energy balances for centralized water heating systems in commercial buildings. To help with future designs, an in-house simulation model of centralized HPWH systems was refined and validated to include natural gas water heater backup. Finally, given the complexity of centralized water heating systems, including recirculation loops, crossover at points of use, and hidden, intricate piping layouts, this project will further explore inexpensive, nonintrusive methods for energy monitoring. These advancements aim to improve the reliability of energy balance calculations, ultimately enabling widespread adoption of efficient, hybrid water heating technologies in commercial buildings.

Field Setup

The mechanical (boiler) room was configured so that building space heating is provided by two natural-gas boilers, each rated at approximately 2 MMBtu/hr. Domestic hot water was originally produced by two natural-gas water heaters; the previous units were defunct 250-gallon heaters rated at 200 kBtu/hr each. When the domestic hot water heaters needed replacement, two 90 kBtu/hr HPWHs were installed to compare the operating costs of HPWH-based water heating with those of the two new 200 kBtu/hr natural-gas water heaters (NGWHs), rated at 95% efficient, equipped with about 110 gallons of storage each (Figure 1).

Figure 1. Boiler room containing two 1 MMBtu/hr boilers, two 90 kBtu/hr high-performance high performance water heaters (HPWHs), and two 200 kBtu/hr natural-gas water heaters (NGWHs) with 110-gallon storage tanks.

In the new system, domestic hot water is generated by a centralized plant that pairs two air-source HPWHs (HPWH 1 and HPWH 2; Figure 2) with two natural-gas water heaters (NG 1 and NG 2; Figure 2). A valve network allowed the equipment to be operated in parallel, in series, or in mixed configurations for testing. Only the configuration in Figure 2 has been tested as it was the recommended configuration by the manufacturer upon start-up of the system.

The initial selected configuration was: city cold water enters NG 1, with HPWH 1 and HPWH 2 connected in parallel with NG 1. From NG 1, water flows to NG 2 and then supplies hot water to the building. The building recirculation return ties into the cold-water line upstream of NG 2 and is directed into bottom of NG 2 via internal dip-tube. In this arrangement, the HPWHs draw from and return to NG 1, maintaining its temperature so that NG 1 did not need to fire.

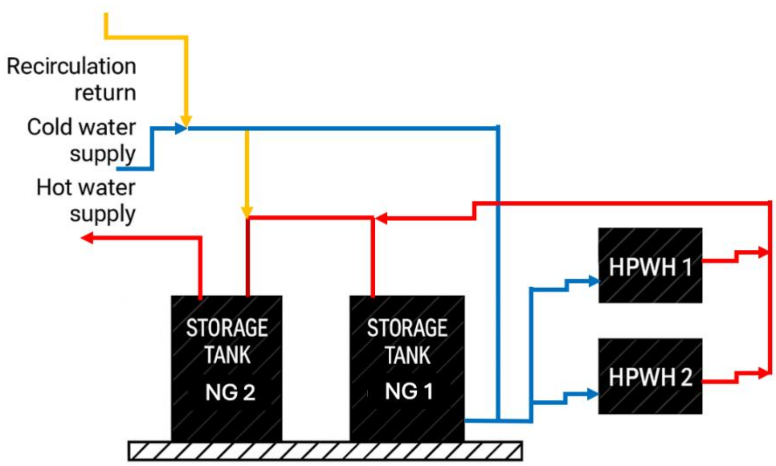

Figure 2. Piping diagram for gas and high performance water heaters that included recirculation return, cold water supply from the city and hot water supply for the building.

Instruments

The system was intentionally over-instrumented with flow meters and temperature sensors to provide redundant measurements and help identify sensor issues or cross-over issues. Cross-over is where cold water and hot water mix in the piping system unintendedly due to a failed fixture in the building. Surface temperature sensors were also included to evaluate whether they could provide sufficiently accurate data for future field-project energy balances.

In total, the instrumentation included five ultrasonic flow meters (each with upstream and downstream surface temperature measurements), sixteen surface thermocouples, and two power meters for the HPWHs (Figure 3). All measured data were transmitted to the building data acquisition and management system for real-time display and long-term recording.

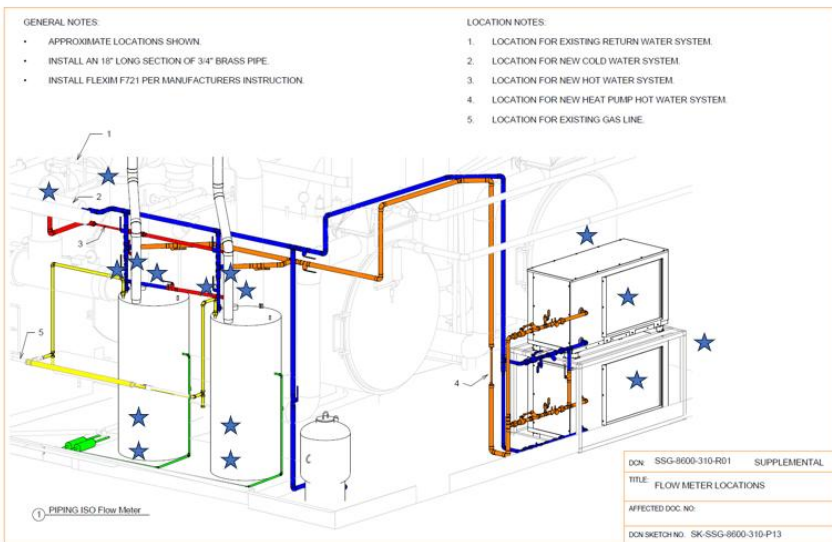

Figure 3. Sensor layout in boiler room. Stars represent surface mount thermocouples and number with arrows show the location of the ultrasonic flow meter installation.

Model

System Configuration and Control

An inhouse central plant water heating model was modified for the configuration shown in Figure 3. The model has been presented at ACEEE Hot Water and Air Forum in 2024 [ref] and at DOE PEER Review 2025 [ref]. The additional updates to the model since those presentations are on the tank stratification and controls which will be discussed in this paper. An air-source HP model (AHP185) with capacity around 185 kBtu/hr was selected for simulation work which represents the two 90 kBtu/hr HPWHs. The natural gas water heater has a capacity of 200 kBtu/hr with 95% efficiency. The tank size is 110 gallons. Each water tank was virtually divided into 6 segments with the same volume (the model details will be introduced in Sub-section 3.3).

As shown in Figure 4, the two natural gas water heaters are named as *NG1* and *NG2*, respectively. *Condenser* denotes the condenser of an air-source HPWH. *Upperband_GAS1* and

Lowerband_GAS1 denote the upper and lower setpoints for gas heating control in *NG1,* based on the temperature measured at the T4 location (approximately at 5/6 of the tank height). The corresponding setpoints are around 65 (60+5)ºF and 55 (60-5)ºF, respectively. *Upperband_GAS2* and *Lowerband_GAS2* denote the upper and lower setpoints for gas heating control in *NG2*. The corresponding setpoints are 130 (120+5) ºF and 125 (120-5) ºF, respectively. *Upperband_HP1* and *Lowerband_HP1* denote the upper and lower setpoints for HPWH heating control in *NG1*, which are around 130 (125+5) ºF and 120 (125-5) ºF, respectively.

$T_{in\_water\_cond}$ and $M_{in\_tank\_NG1}$ mean the condenser inlet water temperature (ºF) and flowrate (gpm), respectively. T_{bot_toHP} and $M_{in\_tank\_NG1}$ mean the temperature and flowrate of water between *condenser* and *NG1*, respectively. $T_{out\_water\_cond}$ is the condenser outlet water temperature (ºF). T_{city} and M_{city} mean the temperature and flowrate of city water, respectively. $T_{in\_tank\_NG2}$ and $M_{in\_tank\_NG2}$ mean inlet mixed water temperature (ºF) and flowrate (gpm) of *NG2*, respectively. T_{con_set} is the set-point of condenser outlet temperature and was varied within the range of 125 to 130ºF. $T_{sup\_building}$ is the temperature of building supply water (ºF) and was fixed at 6.7ºF. $T_{ret\_building}$ denotes the temperature of the building return water (ºF) and was defined as $T_{sup\_building}$ – 6.7ºF. $M_{ret\_building}$ denotes the flowrate of the building return water and was fixed at 8.4 gpm. M_{consu} means the building consumption water flowrate (gpm), it is dynamic and measured on-site. $M_{sup\_building}$ denotes the flowrate of building supply water and was defined as 8.4 gpm + M_{consu}.

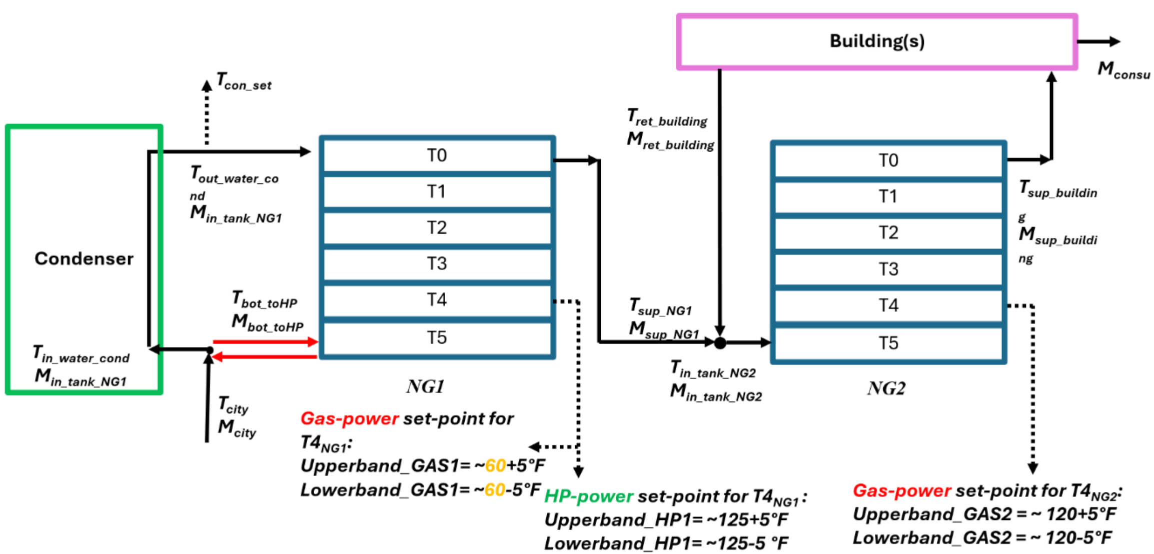

Figure 4. System schematic. From left to right (HPWH condenser, NG1, NG2 and Building)

Air-source HPWH Model

For the air-based HPWH, the evaporator coil undergoes heat exchange with the ambient air via a fan. The indoor fan blows hot air to the evaporator coil. Water flows through the condenser coil to gain heat. The equation is given as follows:

$$Y = a + b \times (T_{air}) + c \times (T_{air})^2 + d \times (T_{wi}) + e \times (T_{wi})^2 + f \times (T_{air}) \times (T_{wi}) \quad (1)$$

Where, T_{air} is the outdoor air temperature (K), T_{wi} is the outdoor air temperature (K), Y is the power consumption (W) or thermal capacity (W). a, b, c, d, e, and f are the coefficients. They can be obtained from water heater manufacturers through a regression fit of the performance data supplied by the manufacturer.

Water Tank Model

The diagram of the water tank model was shown in Figure 4, which is based on the energy balance principle (Nash, Badithela, and Jian 2017; Raccanello and Lazzaretto 2019) and eddy diffusivity (Rendall, 2021). In this study, the water tank was divided into 6 segments with the same thickness.

NG1 and *NG2* have different waterflow configurations. Specifically, as shown in Figure , the hot water (supplied by the air-source HPWHs) comes into the top segment (i.e., T0 segment) of *NG1*. The city water may come into the bottom segment (i.e., T5 segment) of *NG1*. The hot water from the top segment will merge with the building return water, then the mixed water flows into the bottom segment of *NG2*. The building supply water comes from the top segment of *NG2*.

For the top segment of water tank, the generic equation is as follows:

$$C_p M_1 \frac{dT_1}{dt} = c_p m_{in} T_{in} \pm c_p m_{diff} T_{diff} + ES_1 \left[-\frac{k_1 A}{\Delta x} (T_1 - T_2) \right] - hS_1 (T_1 - T_a) - c_p m_{out} T_{out} \quad (2)$$

Where, C_p is the water specific heat (J/kg·k), M_1 is the water mass of the top segment (kg). m_{in} and T_{in} are the inlet water flowrate (gpm) and temperature (K), respectively, which are specially for *NG1* only. m_{diff} and T_{diff} represent the mass flow rate and temperature associated with the mass transfer between adjacent segments. T_{diff} responds to the temperature of the upstream segment (e.g., T_1 or T_2 for the top segment), depending on the flow direction. The magnitude and direction of T_{diff} are determined based on the operating scenario and the mass balance of the tank. Consequently, this term can be either positive or negative in the energy balance, representing heat gain or loss due to inter-segment mass transfer. m_{out} and T_{out} represent the outlet water flowrate and temperature, respectively (Specially, they are M_{sup_NG1} and T_{sup_NG1} for *NG1*, or $M_{sup\_building}$ and $T_{sup\_building}$ for *NG2*, as shown in Figure).

E is the eddy diffusivity. S is the surface area. *h* is the heat convection coefficient between each segment and ambient air T_a (w/m^2·k). *k* is the heat conduction coefficient (W/m·K). *A* is the heat conduction area for each segment (m^2). *Δx* is the thickness of each segment (m).

For the 2nd to the last second segment of water tank, the generic equations are as follows:

$$C_i M_i \frac{dT_i}{dt} = \pm c_p m_{diff} (T_i - T_{i+1}) + \mathrm{E_i} \left[\frac{\mathrm{k_{i-1}\,A_{i-1}}}{\Delta \mathrm{x}} (\mathrm{T_{i-1}} - \mathrm{T_i}) - \frac{\mathrm{k_i\,A_i}}{\Delta \mathrm{x}} (\mathrm{T_i} - \mathrm{T_{i+1}}) \right] - \mathrm{hS_i}(\mathrm{T_i} - \mathrm{T_a}) \quad (3)$$

Where, *i* is the segment index.

For the bottom segment (6th) of water tank, the generic equation is as follows:

$$C_p M_6 \frac{dT_6}{dt} = \pm c_p m_{bot} T_{bot} \pm c_p m_{diff} T_6 + E_6 \left[\frac{k_5\,A_5}{\Delta x} (T_5 - T_6) \right] - hS_6 (T_6 - T_a) \quad (4)$$

Where, m_{bot} and T_{bot} represent the mass flow rate and temperature associated with the water comes into the bottom, respectively (Specially, they are M_{bot_toHP} and T_{bot_toHP} for *NG1*, or $M_{in\_tank\_NG2}$ and $T_{in\_tank\_NG2}$ for *NG2*, as shown in Figure).

Control Algorithm

As shown in Figure 5, a control algorithm was implemented in the simulation to regulate the operation of the HPWHs and the two gas-powered tanks. The algorithm first determines the control sub-loop based on the measured building hot water consumption flow rate (i.e., M_{consu}).

Within each sub-loop, the operating status of the gas heater in *NG2* is determined first. Specifically, the simulated temperature of the target segment in *NG2* (the fifth segment, denoted as $T4_{NG2}$) is compared with the upper and lower setpoints for gas heating (*Upperband_GAS2* and *Lowerband_GAS2*). Based on this comparison, the gas heater status (*NG2_status*) at the current time step is determined.

Next, the operating status of the HPWH (*HP_status*) is determined based on its status in the previous time step and the simulated temperature of the target segment in *NG1* (the fifth segment, denoted as $T4_{NG1}$). The value of $T4_{NG1}$ is compared with the upper and lower HPWH setpoints (*Upperband_HP1* and *Lowerband_HP1*) to determine whether the HPWH should be turned on or off. If the measured building consumption flow rate (M_{consu_mea}) is greater than zero, city water is introduced to compensate for the consumption. Otherwise, the city water flow rate (M_{city}) is set to zero.

It should be noted that, in the current stage of this project, the upper and lower setpoints for gas heating in *NG1* are intentionally set to very low values to effectively disable the gas heating function of *NG1*.

In general, this control strategy ensures that *NG2* primarily maintains the downstream tank temperature, while the HPWH regulates the upstream tank temperature under varying load conditions.

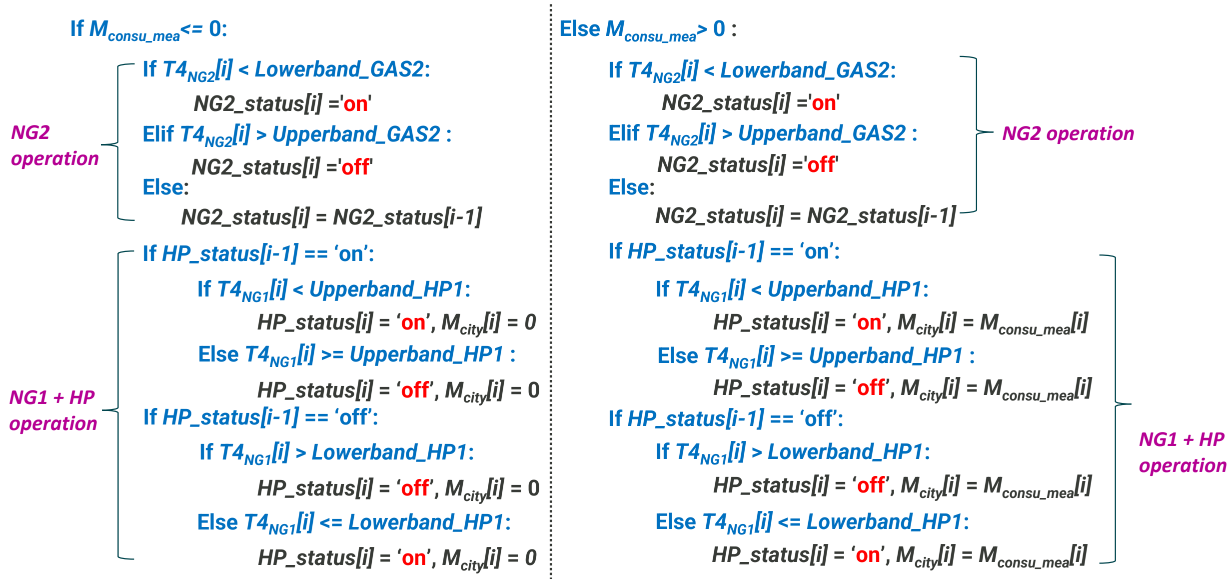

Figure 5. Control algorithm for simulation work. (left) no water is being consumed and (right) water is being consumed by the user and fresh water is entering NG1.

Energy Cost Assumptions

The costs for energy were assumed as the local rate for the city of Oak Ridge, TN of \$0.13/kWh for electricity and \$0.039/kWh (\$1.14/therm) for natural gas. These rates were used to estimate the cost of heating domestic hot water with the HPWHs and the natural-gas (NG) water heaters. Because electricity costs about 3.33 times more per kWh than natural gas, cost parity requires an HPWH coefficient of performance (COP) greater than 3.33.

Results

Sample Model Results

The following figure shows the off-line performance of the whole simulated system on a typical winter day. The historic measured ambient temperature and measured building consumption flow rate (M_{consu_mea}) were used as inputs. *Upperband_HP1* and *Lowerband_HP1* were set as 130(125+5) °F and 120(125-5) °F, respectively. *Upperband_GAS2* and *Lowerband_GAS2* were set as 125(120+5) °F and 111(120-5) °F, respectively. The simulation started at zero clock of a typical day.

In Figure 6, reasonable water stratifications in both water tanks when the HPWH was on, as shown in the subfigures "NG1 temperature profiles" and "NG2 temperature profiles". The HPWH COP with capacity of 185 kBtu/hr can maintain its COP values between 3 to 4, as shown in the sub-figure "Flowrates & Operation/scenarios". Its power consumption was around 12,000 to 14,000 W, as shown in the sub-figure "HP Q & P"

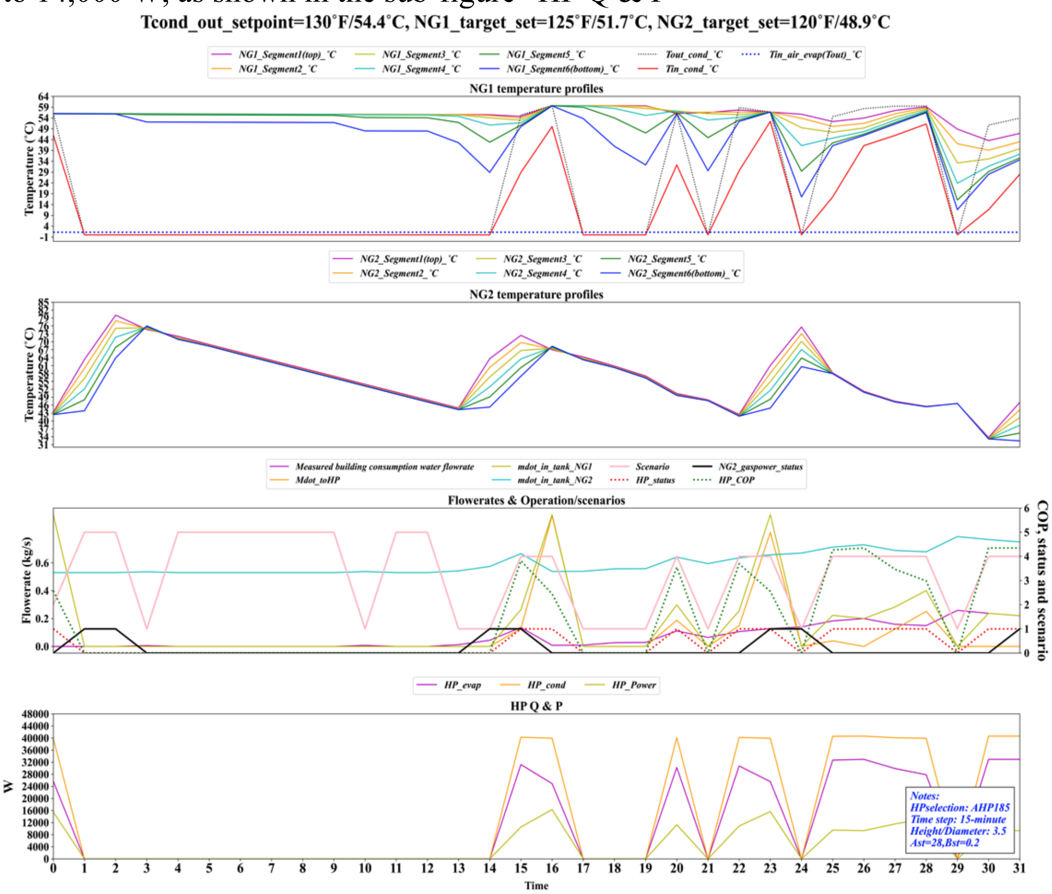

Figure 6. An example of simulation results with time interval of 15-min in winter season.

Sample Field Results

Redundant flow meters and temperature sensors enabled energy balances that quantified both domestic hot-water (DHW) demand and recirculation demand. These loads varied by season and by weekday versus weekend operation. Energy delivered by the HPWHs was directly measured, while natural-gas input was back-calculated from the overall energy balance and the measured demands due to the inability to put an inline flow meter on the gas line. A noninvasive ultrasonic transducer flow meter was installed but did not read accurate values. The cost savings have been run for various NGWH efficiencies (75, 85 and 95%) one might find in the field as a sensitivity study.

In this commercial building, recirculation loads were substantially higher than end-use DHW demand in both fall and winter. Assuming the natural-gas water heaters operate at 95% efficiency, a comparable 95%-efficient electric resistance water heater was used as the baseline for supplying recirculation heat. This allowed the cost impact of different recirculation-heating approaches to be estimated.

Across both seasons (fall and winter), using the natural-gas water heaters to cover recirculation loop heat losses yielded more than 60% cost savings compared with electric resistance heating for the recirculation load due to the cost difference of electricity to natural gas. The HPWH COPwas also calculated (Figure 7). Two control strategies were tried, one for HP domination where the setpoint of the HPWH was set higher 5°F (2.78 °C) than NG2 and one where HPWH was set to the same temperature NG2. For the randomly selected weeks, where there was no big impact to demand around the holiday seasons, in fall and winter 2025–26, the measured COP ranged from 2.7 to 3.8 when using thermal power / volts times amps – notably the power factor was 0.74 on average when running which yields a higher COP when real power is used in the denominator of the COP calculation. This indicates that, in this climate, a control strategy that prioritizes the HPWHs in the winter minimizes operating cost. In colder climates (with cooler mechanical rooms) or where winter natural-gas prices are lower, a strategy that relies more on the NG water heater may be needed to reduce costs.

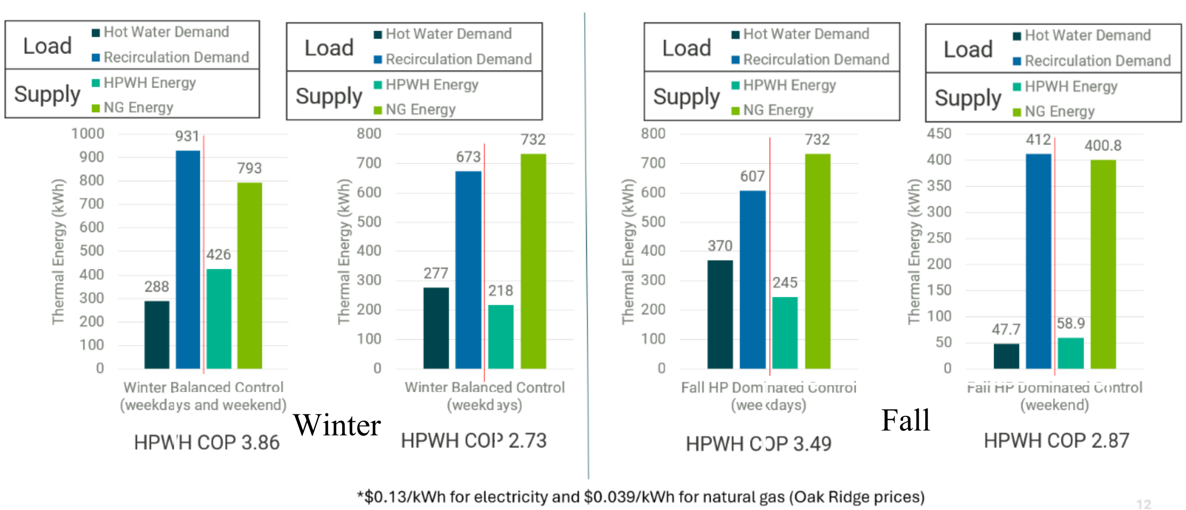

Figure 7. Results of random fall and winter weeks for user hot water demand, thermal recirculation loss demand, HPWH energy and NG energy added to the water with cost savings including HPWH and system COP. Please note, the flowrate mismatch of the recirculation line and hot water line was noticed in the winter which is assumed cross-over event where the calculated COP may be off due to warming of the cold water line.

Yearly cost savings can be estimated by comparing a swing-tank system using electric resistance heating against the hybrid NG + HPWH installation. Using the two seasons of experimental results together with the validated model to measured HPWH COP within 10%, runtime within 30% and total energy use with 15% annual operating costs were projected from the experimental data over the sampled weeks. Please note, the runtime was limited in the data collection as the HPWHs often short cycled, due to minimal storage volume, to a 15 minute run and the time collection was at a 15 minute time stamp so often the runtime was double counted in the experimental data. The resulting yearly cost savings are significant when compared to natural gas performance at 95% ($6,830 savings), 85% ($6360 savings) and 75% ($5760 savings) , as shown in Figure 8.

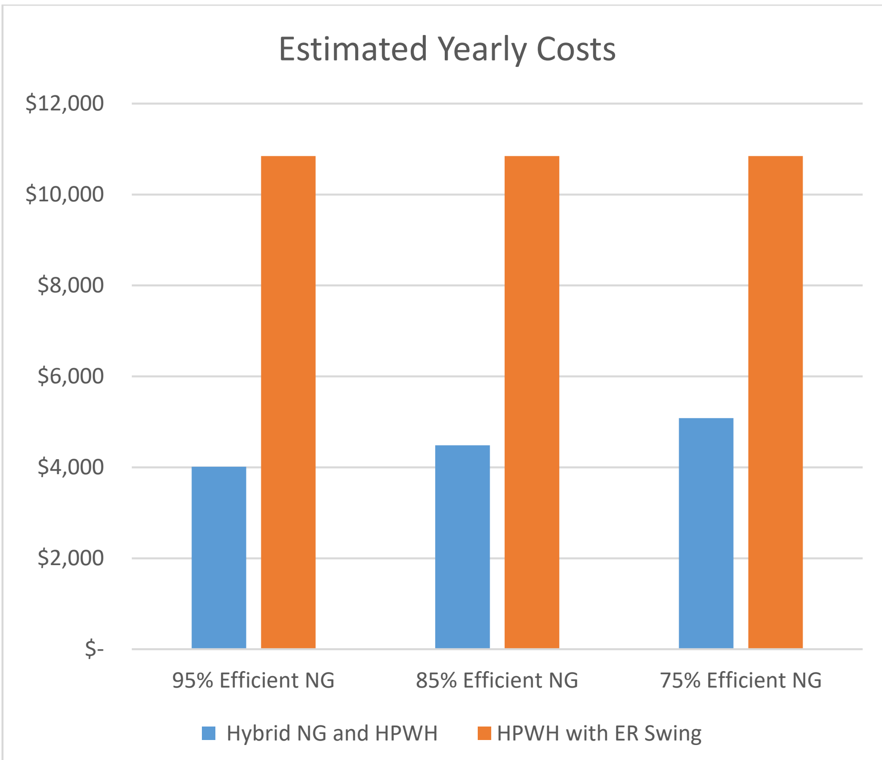

Figure 8. Predicted yearly cost savings for installing a natural gas water heater at the swing tank instead of an electric resistance heater for this commercial installation in Oak Ridge, TN.

Instrumentation Analysis

Another project goal was to determine how many sensors are required for a good energy balance for HPWHs in the field. Thus the system was first over instrumented and only the critical sensors for the HPWH energy balance and for error state identification were used in the final analysis. Analysis of data from the 16 thermocouples and five flow meters showed that the instrumentation set could be reduced to eight thermocouples and three flow meters without sacrificing the key energy-balance and diagnostic capabilities. Power monitoring of the HPWHs is still required (Figure 9).

The cold-water inlet does not need to be metered directly because the redundant flow meters on the recirculation loop allow cold-water make-up to be inferred from the difference between the measured flows. This redundancy also enables detection of hot/cold cross-over during periods of no draw: when there is no end use (e.g., at night) or when the cold-water supply is temporarily shut off, the two recirculation-related meters should read the same flow. Any persistent difference indicates a mass imbalance and implies that water is leaking or being driven into the cold-water system.

In this project cross-over was identified by the "typically considered" redundant flow meters on the recirculation line and hot water line. After the space heating boilers, located in the same room, were updated, the measured leaving hot-water flow rate was lower than the returning flow rate during periods of noflow, indicating that the recirculation pump was pushing return water into the cold-water piping or the flow meters had been bumped during the space heating boiler upgrades. The opposite situation, leaving hot-water flow lower than return flow in a different pattern, could indicate cold water being pulled into the hot-water system or hot water being pushed into cold lines somewhere in the building. In this case, the most likely explanation is that return water forced into the cold-water line was being consumed by the space heating boilers through a faulty check valve or the flow meters were bumped during the work in the boiler room.

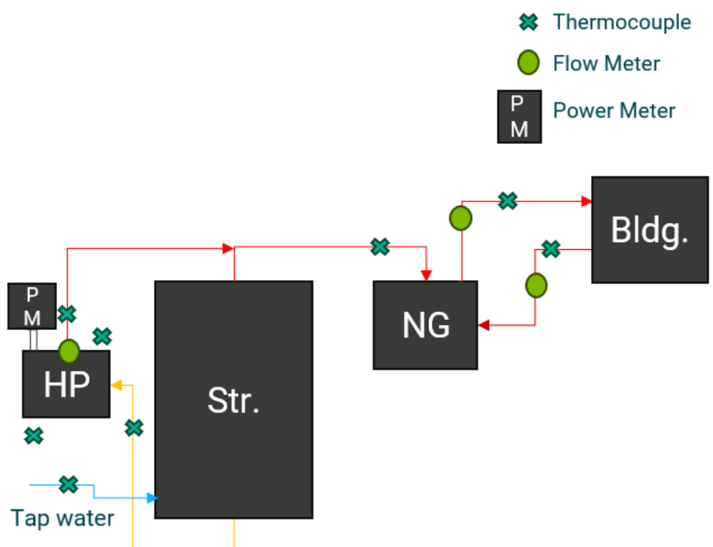

Figure 9. Minimal sensor requirements for energy balance of centralized water heating system with HP and NG water heaters that include hot water storage (Str.). Air-side HP sensors are not required but are good to compare to manufacturer data sheets on performance.

The temperature sensors can be reduced to eight for HPWH performance measurement. If the goal is to measure NG efficiency, then a flow meter the gas line is required and combustion instrumentation is required for the highest accuracy energy balance. Although the air-side temperature measurements are not used in the energy balance, they are useful for comparing water-heater performance against manufacturer specifications.

Six thermocouples, used with three flow meters, are sufficient to quantify hot-water energy consumption, return-water energy consumption, and HPWH performance by monitoring the inlet and outlet temperature differences at the tank surface. Because the thermal lag of the surface measurements is similar during HPWH startup and shutdown, using the inlet–outlet temperature difference largely compensates for thermal-lag effects. Likewise, during cold-water draws, the thermal lag is consistent between the inlet and outlet measurements on the storage tank, so the inlet–outlet temperature difference remains representative of delivered heat. For the recirculation lines, flow is continuous and the system is typically near steady state, which further simplifies the energy-balance calculations.

Conclusions

This project demonstrated that a hybrid centralized domestic hot water system combining HPWHs with natural gas water heaters (NGWHs) can be operated effectively in a commercial building using simple setpoint-based control. By selecting appropriate setpoints and locating HPWHs in warm mechanical-room conditions, the system maintained high winter performance (measured COP was roughly 2.7-3.8) and achieved at least a 60% cost reduction compared with conventional HPWH systems that rely on electric resistance backup. Increasing HPWH time-out settings enabled longer run cycles (≥20 minutes) and showed that a single HPWH could meet the heating demand under tested conditions, indicating potential for reduced equipment counts in future designs. The study further identified a practical path to lower-cost monitoring by reducing instrumentation to a minimal set (approximately three flow meters, eight temperature sensors, and HPWH power metering) and introduced a crossover detection method to identify hidden piping and flow issues.

Key limitations were identified that inform future installations: insufficient storage volume constrained stable operation and contributed to short cycling, while gas-flow measurement remained a challenge due to the inability of water-designed ultrasonic flow meters to accurately measure natural gas. Overall, the work supports the viability of hybrid HPWH–NGWH systems for commercial centralized water heating, while emphasizing that proper storage sizing, improved commissioning to reduce short cycling, and robust low-cost monitoring methods are essential for dependable performance verification and broad adoption.

Next steps include future designs for the field that reduce HWPH size and increase storage, fixing the identified cross-over issue, and replacing the NG flow meter. Setpoint changes to determine impact in spring and summer that includes model validation for these seasons.

Acknowledgements

This work was supported by the US Department of Energy (DOE), Office of Critical Minerals and Energy Innovation's Building Technologies Office (BTO) Commercial Building Integrations IMPACT project. The installation was funded by Oak Ridge National Laboratory's Facilities and Operations Directorate. Resources from the Building Technologies Research and Integration Center, a DOE-designated national user facility operated by Oak Ridge National Laboratory, were also used.

AI-assisted tools used: Chat GPT 5.2
Used for: copyediting and summarizing research log
Extent: editing
Human review: The authors reviewed and verified all content, calculations, and citations.

References

EIA. (2023a). 2020 Residential Energy Consumption Survey Data. US Energy Information Administration. https://www.eia.gov/consumption/residential/data/2020/ Feb 28 from https://www.eia.gov/outlooks/aeo/.

Malhotra, M., Krishnan, E., Rendall, J., Casey, F., Li, Y., Nawaz, K., Sun, J., Brechtl, J., Worek, W. and Klein, G., 2024. Cost Reduction of Het Pump Water Heating in Cold Climates for Low to Moderate Income Families. Oak Ridge National Laboratory (ORNL), Oak Ridge, TN (United States).

Nash AL, Badithela A, Jain N. Dynamic modeling of a sensible thermal energy storage tank with an immersed coil heat exchanger under three operation modes. Applied Energy 2017;195:877–89.

NEEA, Northwest Energy Efficiency Alliance Advanced Water Heating Specification, Version 8.1, https://neea.org/wp-content/uploads/2025/03/Advanced-Water-Heating-Specification.pdf, Sampled 3/11/2026

Raccanello J, Rech S, Lazzaretto A. Simplified dynamic modeling of single-tank thermal energy storage systems. Energy 2019;182:1154–72.

Rendall, J., Karg-Bulnes, F., Gluesenkamp, K., Abuheiba, A., Worek, W., and Nawaz, K., "A flow-rate dependent 1D model for thermally stratified hot-water energy storage," Energies 14(9), 2661, 2021.

Steven Winter Associates, Inc., 2019, "Het Pump Retrofit Strategies for Multifamily Buildings". https://basc.pnnl.gov/library/heat-pump-retrofit-strategies-multifamily-buildings.